

EdgeNet: Semantic Scene Completion from RGB-D images

Aloisio Dourado, Teofilo Emidio de Campos
University of Brasilia
Brasilia, Brazil

t.decamos@st-annes.oxon.org

Hansung Kim, Adrian Hilton
University of Surrey
Surrey, UK

(h.kim, a.hilton@surrey.ac.uk)

Abstract

Semantic scene completion is the task of predicting a complete 3D representation of volumetric occupancy with corresponding semantic labels for a scene from a single point of view. Previous works on Semantic Scene Completion from RGB-D data used either only depth or depth with colour by projecting the 2D image into the 3D volume resulting in a sparse data representation. In this work, we present a new strategy to encode colour information in 3D space using edge detection and flipped truncated signed distance. We also present EdgeNet, a new end-to-end neural network architecture capable of handling features generated from the fusion of depth and edge information. Experimental results show improvement of 6.9% over the state-of-the-art result on real data, for end-to-end approaches.

1. Introduction

The ability of reasoning about scenes in 3D is a natural task for humans, but remains a challenging problem in Computer Vision [16]. Knowing the complete 3D geometry of a scene and the semantic labels of each 3D voxel has several applications, like robotics, surveillance, assistive computing, augmented reality and many others.

Currently, there is a wide availability of low cost RGB-D sensors, but those sensors generate $2\frac{1}{2}$ D images from a specific viewpoint, rather than complete 3D scene data. In other words, they generate data from a single viewing pose and cannot handle occlusion among objects in the scene nor the fact that their field of view is restricted. The volumetric data that can be generated directly from depth sensors is therefore incomplete and sparse. For instance, in the scene depicted on the left part of Figure 1, parts of the wall, floor and furniture are occluded by the bed. There is also self-occlusion: the interior of the bed, its sides and its rear surfaces are occluded by its visible surface.

Given a partial 3D scene model generated from a single RGB-D image, the goal of scene completion is to generate a complete 3D voxelized volumetric representation where

each voxel is labelled as occupied by some object or free space. In addition, for occupied voxels, the goal of *semantic* scene completion is to assign a label that indicates to which class of object it belongs, as shown on the right part of Figure 1.

Before 2018, most of the work on scene reasoning only partially addresses this problem. A number of approaches only infer labels of the visible surfaces [10, 19, 18], while others only consider completing the occluded part of the scene, without semantic labelling [5]. Another line of work focuses on single objects, without the scene context, e.g. [17].

The term semantic scene completion was introduced by Song *et al.* [25], who showed that scene completion and semantic labelling are intertwined and training a CNN to jointly deals with both tasks can lead to better results. To deal with the sparsity of the 3D data gathered from depth maps, Song *et al.* used a variation of Truncated Sign Distance Function (TSDF) to encode the 3D occupancy grid. Their work only used the depth information, ignoring all information from RGB channels.

Colour information is expected to be useful to distinguish objects that approximately share the same plane in the 3D space, and thus, are hard to distinguish using only depth. Examples of such instances are flat objects attached to the wall, such as posters, paintings and flat TVs. Opaque windows also pose a problem for depth-only approaches.

Recent research on scene completion also explored the use of the colour information present on RGB-D images to improve Semantic Scene Completion [6, 7]. However, these methods project colour information in a naive way, leading to a problem of data sparsity in the voxelised data that is fed to the 3D CNN.

Our work focuses on semantic scene segmentation using depth and colour. In order to address the RGB data sparsity issue, we introduce a new strategy for encoding information extracted from RGB image after projection from 2D to 3D. We also present and evaluate a new end-to-end 3D CNN architecture to deal with all the features gathered after fusion of colour and depth. We propose a lightweight frame-

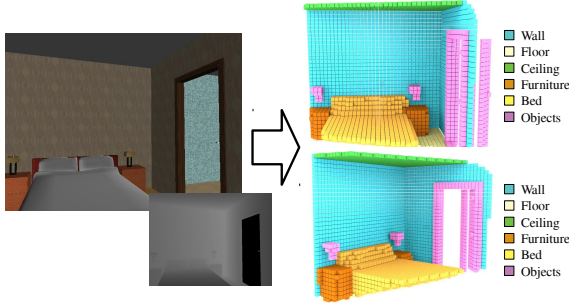


Figure 1: Semantic scene completion. Given an RGB-D image, the goal is to infer a complete 3D occupancy grid with associated semantic labels. For instance, part of the furniture is occluded by the bed, but its 3D reconstruction should handle occlusions.

work and pipeline to train deep 3D semantic scene completion CNNs with lower memory and time requirements than previous implementations. Comprehensive experiments are conducted to evaluate the proposed solution. Results show that our solution is superior to previous works.

To summarise, our main contributions are:

- a new strategy for encoding colour into a 3D volume to address the sparsity problem of RGB data;
- a new end-to-end convolutional network architecture that benefits from the fusion of depth and colour for semantic scene segmentation;
- a lightweight framework to train deep 3D CNNs.

2. Related Work

Scene Semantic Completion (SSC) in 3D is a problem that was established quite recently and has a high computational cost due to the volume of 3D data. Most works on 3D SSC rely on Fully Convolutional Neural Networks architectures (FCNs, introduced in [15]) and use SUNCG and NYUv2 as training sources (these datasets are described in Section 5.1). We classify approaches into three main groups, based on the type of input of the semantic completion CNN: depth maps only, depth maps plus RGB and depth maps plus 2D segmentation maps.

2.1. Depth maps only

Song *et al.* [25] used a large synthetic dataset (SUNCG) to generate approximately 140 thousand depth maps that were used to train a typical contracting fully convolutional CNN with 3D dilated convolutions, called SSCNet. They showed that jointly training for segmentation and completion leads to better results, as both tasks are inherently intertwined. To deal with data sparsity after projecting depth

maps from 2D to 3D, the authors used a variation of Truncated Signed Distance Function (TSDF) that they called Flipped TSDF (F-TSDF). See Section 3 for a detailed explanation on F-TSDF. As the ratio of empty vs. occupied voxels is around 9:1, to compensate this data imbalance, SSCNet uses a weighted softmax loss function where, for each training volume containing N occupied voxels, $2N$ empty voxels were randomly selected from occluded regions to be assigned a $weight = 1$. Voxels in free space, outside the field of view, or outside the room are assigned $weight = 0$. Occupied voxels are assigned $weight = 1$. After training on synthetic data, SSCNet was fine tuned on NYU. Results were also reported training from scratch on NYU and using a model trained on SUNCG and evaluating on NYU with no fine tuning.

Zhang *et al.* [27] used Spatial Group Convolution (SGC) and a U-Net shaped network [20] for accelerating the computation of 3D dense prediction. SGC was used in the encoding branch of the U-Net, while regular 3D convolutions and 3D transposed convolutions were used in the decoding branch. The authors also used F-TSDF to encode the projected depth map, and the same weight strategy as [25]. Zhang *et al.* trained their model from scratch on SUNCG and on NYU and did not fine tune it. The authors reported good results on synthetic data but got results equivalent to SSCNet on real data.

Guo and Tong [9] applied the depth map to a sequence of 2D convolutions, then projected the generated features to 3D using a projection layer, before applying them to a 3D CNN. They trained their model on SUNCG and fine tuned on NYU. Unfortunately they evaluate the results every 2000 steps after 130K iterations, and averaged them as final result, which means that their reported results are not from single models.

2.2. Depth maps plus RGB

Guedes *et al.* [7] reported preliminary results obtained by adding colour to an SSCNet-like architecture [25]. In addition to the F-TSDF encoded depth volume, they used three extra projected volumes, corresponding to the channels of the RGB image, with no encoding, resulting in 3 sparse cubes. The authors reported no significant improvement using the colour information in this sparse manner.

2.3. Depth maps plus 2D segmentation

Models in this category use a two step training protocol, where a 2D segmentation CNN is first trained and then it is used to generate input to a 3D semantic scene completion CNN. Current models differ in the way the generated 2D information is fed into the 3D CNN.

Garbade *et al.* [6] used a pre-trained 2D segmentation CNN with a fully connected CRF [4] to generate a segmentation map, which, after post processing, was projected to

3D. In order to save memory, the authors did not use one-hot-encoding, instead, class labels were projected. Training the 2D CNN was done offline. They used four datasets for training: SUN-RGBD [24], Berkeley B3DO [13] and SUN3D [26], as well as NYU. Their 3D CNN architecture is similar to SSCNet, except for the input layers, which comprise the F-TSDF encoded depth map and the three volumes generated from the segmentation map.

Liu *et al.* [14] used depth maps and RGB information as input of an encoder-decoder 2D segmentation CNN. The encoder branch of the 2D CNN is a ResNet-101 [12] and the decoder branch contains a series of dense upsampling convolutions. The generated features from the 2D CNN are then reprojected to 3D using camera parameters, before being fed into a 3D CNN. The authors showed results using 2 different strategies to fuse depth and RGB: SNetFusion perform fusion just after the 2D segmentation network, while TNetFusion only performs fusion after 3D convolutional network. TNetFusion achieves higher performance with the cost of having higher computational costs. The 2D CNN is also pre-trained offline.

Using 2D segmentation maps on 3D SCC brings an additional complexity to the training phase which is training and evaluating the 2D segmentation network prior to the 3D CNN training. In this work, we focus on end-to-end approaches, where the whole network can be trained and evaluated as a whole.

3. Representing edges in 3D

As discussed earlier, colour information should complement depth maps for 3D Semantic Scene Completion (SSC), however it is not trivial how these modalities should be combined. Guedes *et al.* [7] naively added 3 channels to each voxel to insert R, G and B colour information into the representation, with no encoding. In this way, the vast majority of voxels have no colour data while only those at the visible surface have a colour value. This explains why their results are not better than the original method of Song *et al.* [25]. Song *et al.* have shown that F-TSDF encoding plays an important role in feeding a projected depth map to a 3D CNN.

Given a sparse 3D voxel volume, the Truncated Signed Distance Function (TSDF) consists of computing the Euclidean distance of each empty voxel to the nearest occupied voxel. The signal of occluded regions is set to be negative, while visible regions are given positive values. Near the occupied surface, TSDF produces a value that tends to zero on both sides (and its first derivative tends to zero, as well). TSDF values are normalised to (-1,1). Flipped TSDF (F-TSDF) follows the same principle, but the absolute values of both visible and occluded regions are flipped, as stated in Equation 1. F-TSDF produces a discontinuity near the occupied surface (from -1 to 1), and the first derivative tends

to infinite, in opposition to TSDF.

$$F-TSDF = \text{sign}(TSDF) \cdot (1 - |TSDF|) \quad (1)$$

Song *et al.* [25] has shown that F-TSDF encoding of volumetric data produces better results than TSDF and other encoding techniques, however, while F-TSDF can be easily applied to depth maps after 3D projection, it can not straightforwardly be applied to RGB nor semantic segmentation maps. Regarding depth maps after 3D projection, each voxel carries a binary information: occupied or free space and, as so, F-TSDF can be used. This is not the case for RGB or semantic segmentation maps, because they are not binary.

To deal with this problem, we introduce a new strategy to fuse colour appearance and depth information for 3D SSC. Our approach consists on detecting edges in the image, which gives a 2D binary representation of the scene that can highlight flat objects on flat surfaces. For instance, a poster on a wall is expected to be invisible in a depth map, especially after down-sampling. On the other hand, RGB edges highlight the presence of that object. We use the standard Canny edge detector [3] to perform edge detection. Each edge location is projected to a point in the 3D space using its depth information and the camera calibration matrix. The resulting point cloud is voxelised in the same way as the depth point cloud, resulting in a sparse volume of 240 x 144 x 240 voxels. Figure 2 shows a scene from SUNCG dataset and its corresponding edges projected to 3D.

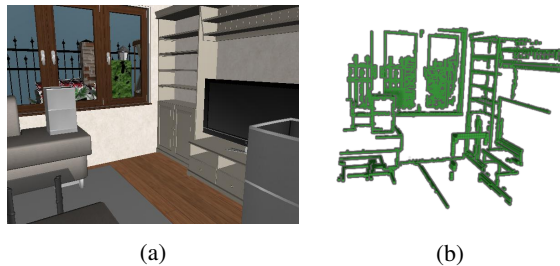


Figure 2: Projection of Edges to 3D: (a) original RGB image, (b) voxelized edges after projection.

The main advantage of extracting edges and projecting them to 3D is the possibility to apply F-TSDF on both edges and surface volumes, as they are both binary, thus providing two meaningful input signals to the 3D CNNs. Figure 3b shows in detail a region of the projected edges of 3a after F-TSDF encoding. Note that the greater gradients occur along the edges.

3.1. Preprocessing the data to speed up training

The SUNCG dataset contains more than 130K 3D scenes samples. In order to train a single model, each scene is processed several times, according to the number of epochs

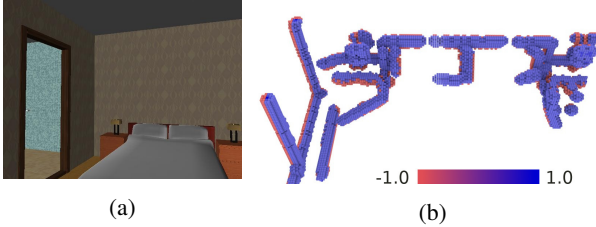


Figure 3: F-TSDF applied to projected edges: (a) original scene, (b) F-TSDF of edges in 3D. Edges image is an horizontal cut of the scene, taken just above the bed. Only F-TSDF values with absolute value greater than 0.8 are shown. Note in the center of the cut of the door frame, the high gradient that occurs along the edge (best viewed in colour).

used. As F-TSDF calculation is computationally intensive, to reduce overall training time, the F-TSDF volumes that feed the models are preprocessed off-line once. The pre-processed dataset is then stored, and may be used as many times as needed, including by different models. Following [25] we rotate the 3D Scene to align with gravity and room orientation based on the Manhattan assumption. We fixed dimensions of the 3D space to 4.8 m horizontally, 2.88 m vertically, and 4.8 m in depth. Voxel grid size is 0.02 m, resulting in a $240 \times 144 \times 240$ 3D volume. TSDF truncation value is 0.24 m. Surface and edge projection as well as F-TSDF encoding of all volumes are done in this stage.

During preprocessing, we also calculate an occupancy grid where we distinguish occupied voxels inside the room and FOV, non-occupied occluded voxels inside the room and FOV, and all other voxels. This occupancy grid will be further used to balance the dataset during training time.

By running all these steps in a preprocessing stage, our framework avoids the excessively redundant processes of the original SSCNet architecture, which implements these steps as part of the first layer of their neural network. Their framework is not only slower but also requires much more GPU memory.

4. EdgeNet

In order to better capture and aggregate information from both depth and edges, we present a new 3D Semantic Segmentation CNN that we call **EdgeNet**. Our proposed network architecture is a deeper 3D CNN inspired by the U-Net design [20] which has been successfully used in many 2D semantic segmentation problems, and is presented in Figure 4. We address the degradation problem of deeper networks, by replacing simple convolutional blocks of U-Net by ResNet modules [12]. To match the resolution of the output, the first 2 stages reduce the resolution to 1/4 of the input. Next blocks follows encoder-decoder design and,

following [25], we used dilated convolutions on lower resolutions to improve the receptive field. The last stage is responsible for reducing the number of channels to match the desired number of output classes and loss calculations.

In volumetric data, occluded and occupied voxels are highly unbalanced, so we use a weighted version of categorical cross entropy as the loss function to train our models. To obtain the weights, for each training batch, we randomly initialize a tensor $rand_{occl}$ of the same shape as the batch with ones and zeroes using the ratio $r = (2 \sum occu / \sum occl)$, where $occl$ and $occu$ are two tensors obtained from the previously calculated occupancy grid relative to occluded and occupied voxels. The final weight tensor is $w = occu + occl \odot rand_{occl}$, where \odot denotes the Hadamard product. This produces the same effect as the random selection of occluded voxels used in [25], but in a more efficient way.

Let p be the predicted probabilities of the 12 classes for each voxel and y be the one hot encoded ground truth tensor. The categorical cross entropy loss function is then given by equation 2.

$$L_{cce}(p, y) = - \sum (w \odot y \odot \log p) \quad (2)$$

4.1. Extra models for comparison purposes

In order to properly assess the effect of aggregating edges to the input and also to evaluate the effect of using a deeper U-shaped CNN, we take **SSCNet** [25] as a baseline shallower CNN without edges and report the results from the original paper. We also propose two other models for an ablation study of components of EdgeNet. The first is **E-SSCNet**, a modified version of SSCNet that takes as input F-TSDF encoded edge volume concatenated to the original depth volume. We also evaluate a modified version of our EdgeNet without the aggregated edge volume. We call that version **U-SSCNet**, as a reference to the U-shaped design. All our models were developed using Tensorflow. To evaluate the effect of our training pipeline and the use of preprocessing steps discussed in Section 3.1, we ported the SSCNet to Tensorflow and trained it with the same hyper parameters and loss function as our other models. This version is referenced in this paper as **SSCNet***.

4.2. Training protocols

Our experiments consists in training our models from scratch on SUNCG and NYU, and also fine-tuning models trained on SUNCG on NYU (these datasets are described in Section 5.1).

For experiments in which we trained our models from scratch, we use the technique known as One Cycle Learning [22], which is a combination of Curriculum Learning [2] and Simulated Annealing [1]. After some preliminary tests, we found 0.01 to be a good base learning rate. This value

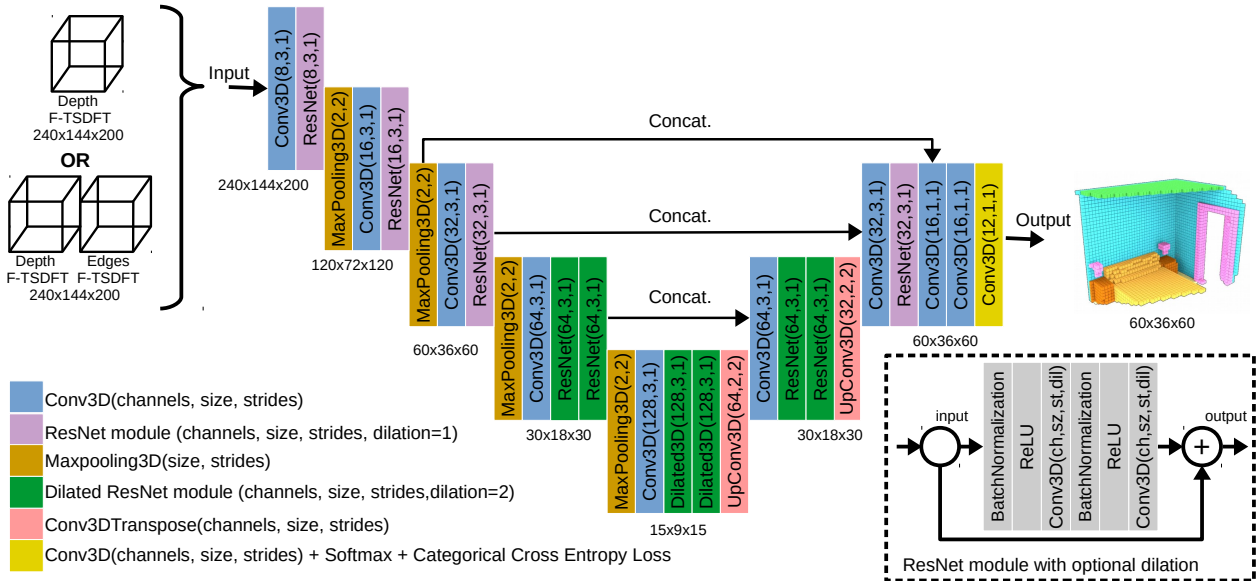


Figure 4: The proposed U-shaped architecture with two possible sets of input channels: the proposed EdgeNet, which uses depth and edges, and U-SSCNet, which has the same architecture but uses only depth as input (best viewed in colour).

is also used in several recent works on the same datasets [25, 7, 9, 6, 14]. We use a maximum of 30 epochs, in order to maintain total training time in a acceptable limit. Following [22], we start with the base learning rate and linearly increase the effective learning until 0.1 in the 10th epoch, then linearly decrease the learning rate until reach the start-up level in the 20th epoch. During the annealing phase, we linearly go from 0.01 to 0.0005 in a further 10 epochs.

Due to GPU memory size, we use a batch with 3 samples. We also used SGD optimizer with a momentum of 0.9 and decay of 0.0005 in all experiments as used in most previous works. For SUNCG, each epoch consists of 30,540 scenes randomly selected from the whole training set. For NYU, each epoch comprises the whole dataset.

For fine tuning, we initialize the network with parameters trained on SUNCG and use standard training with SGD with fixed learning rate of 0.01 and 0.0005 of weight decay.

Thanks to our lightweight training pipeline with offline F-TSDF preprocessing, our training time is only 4 days on SUNCG and 6 hours on NYU, using a GTX 1080 TI.

5. Experiments

In this section we describe the datasets and the evaluation protocol used in this paper.

5.1. Datasets

We train and validate our proposed approach on SUNCG [25] and NYUv2 [21] datasets. SUNCG dataset consists of about 45K synthetic scenes from which were extracted more than 130K 3D scenes with corresponding depth maps

and ground truth divided in train and test datasets. Original provided data was extracted from SUNCGv0, and did not include RGB images. So we downloaded the currently available version of SUNCG (SUNCGv1) and used the provided camera information for each scene and provided toolbox to generate corresponding RGB images of each scene. The same ground truth and depth maps as [25], are used for fair comparison of results.

NYUv2 dataset includes depth and RGB images captured by the Kinect depth sensor divided in 795 depth images for training and 654 for test. Following the majority of works in semantic segmentation we used ground truth by voxelizing the 3D mesh annotations from [8] and mapped object categories based on [11].

5.2. Evaluation

We follow exactly the same evaluation protocol as [25], with the same test datasets. For the semantic scene completion task, we report the IoU of each object class on both the observed and occluded voxels. For the scene completion task, all non-empty object classes are considered as one category, and we report Precision, Recall and IoU of the binary predictions on occluded voxels. Voxels outside the view or the room are not considered.

6. Results

In this section we report quantitative results of EdgeNet on NYUv2 and compare them to other end-to-end approaches. We also present and compare results of alternative models to our proposed approach, in order to investigate

train	input	model	scene completion		semantic scene completion (IoU, in percentages)												
			prec.	rec.	IoU	ceil.	floor	wall	win.	chair	bed	sofa	table	tv	furn.	objs.	avg.
SUNCG	d	SSCNet[25]	55.6	91.9	53.2	5.8	81.8	19.6	5.4	12.9	34.4	26	13.6	6.1	9.4	7.4	20.2
	d+e	EdgeNet(Ours)	59.4	84.3	53.5	4.7	88.1	15.0	5.3	13.8	42.5	28.5	8.8	3.0	12.5	9.7	21.1
NYU	d	SSCNet[25]	57.0	94.5	55.1	15.1	94.7	24.4	0.0	12.6	32.1	35.0	13.0	7.8	27.1	10.1	24.7
		SGC[27]	71.9	71.9	56.2	17.5	75.4	25.8	6.7	15.3	53.8	42.4	11.2	0.0	33.4	11.8	26.7
	d+e	EdgeNet(Ours)	78.4	66.2	56.0	19.7	94.9	28.1	0.0	7.5	52.5	41.8	10.4	0.0	34.7	12.8	27.5
SUNCG +NYU	d	SSCNet[25]	59.3	92.9	56.6	15.1	94.6	24.7	10.8	17.3	53.2	45.9	15.9	13.9	31.1	12.6	30.5
	d+c	Guedes <i>et al.</i> [7]	-	-	56.6	-	-	-	-	-	-	-	-	-	-	-	30.5
	d+e	EdgeNet(Ours)	76.3	71.1	58.3	23.6	95.0	28.6	12.6	13.1	57.7	51.1	16.4	9.6	37.5	13.4	32.6

Table 1: **Semantic scene completion results of end-to-end approaches on NYU test set.** Column ‘input’ indicates the type of input: d=depth only; d+e=depth and edges. Column ‘train’ indicates dataset used for training the models. SUNCG + NYU means trained on SUNCG and fine tuned on NYU. EdgeNet presented the best results on all training scenarios.

input	model	scene completion		semantic scene completion (IoU, in percentages)												
		prec.	rec.	IoU	ceil.	floor	wall	win.	chair	bed	sofa	table	tv	furn.	objs.	avg.
d	SSCNet[25]	76.3	95.2	73.5	96.3	84.9	56.8	28.2	21.3	56.0	52.7	33.7	10.9	44.3	25.4	46.4
	SSCNet*	86.7	90.9	79.8	98.0	87.5	59.8	34.7	34.5	73.5	65.2	44.4	26.4	52.1	40.0	56.0
	U-SSCNet	86.8	93.5	81.8	98.2	89.7	61.0	47.3	45.5	79.6	71.1	52.9	28.7	64.9	52.7	62.9
d+e	E-SSCNet	86.2	91.3	79.6	98.2	87.7	59.3	35.4	35.4	74.2	64.7	45.4	25.9	54.1	41.3	56.5
	EdgeNet	86.9	93.2	81.8	98.3	89.7	61.1	47.6	45.5	79.9	72.1	51.8	33.1	64.2	51.7	63.2

Table 2: **Ablation study on SUNCG test set.** Column ‘input’ indicates the type of input: d = depth only; d+e = depth + edges. SSCNet* is our implementation of the original SSCNet architecture trained with our pipeline.

effects of components of our solution using the SUNCG dataset. Qualitative results are also provided.

6.1. Results on NYU

Table 1 shows the results of EdgeNet on NYUv2 dataset and compare them to recent end-to-end semantic scene completion approaches, for models trained only on synthetic data, only on NYU and on both synthetic and NYU using fine tuning. We present results extracted from their original papers. Overall, EdgeNet achieved the best scores on each one of the training scenarios, improving the state-of-art on 3D SSC on NYU. Considering training on SUNCG and fine tuning on NYU the improvement was 3% on scene completion and 6.9% on semantic scene completion.

6.2. Results of our models on SUNCG

Table 2 shows the results of variations of EdgeNet on SUNCG dataset to investigate the effect of aspects of our proposed solution over model performance. On both depth only and depth plus edges approaches, the deeper network presented better results.

Comparing both deeper networks, (U-SSCNet and EdgeNet), the version that also receives edges as input achieved better results, but improvement was observed only

on semantic scene completion. Same situation occurred to shallower networks (SSCNet and E-SSCNet), where the version with depth plus edges was better on SSC.

Comparing the original SSCNet and its version trained with our pipeline (SSCNet*), there were improvements in all metrics except recall.

6.3. Qualitative Results

Qualitative results on NYU are shown in Figure 5 and overall corresponding scores are presented on Table 3. Models used to generate the inferences were trained on SUNCG and fine tuned on NYU. We compare results of SSCNet* to our three models. We used the same scenes presented on qualitative results of [25]. It is visually perceptible that EdgeNet presents the best results.

In the first row of images of Figure 5, note how EdgeNet correctly captures the details of the laptop and other small objects on the table. The effect of the use of edges over flat objects is made clear on the forth row. While SSCNet and U-SSCNet are incapable of distinguishing the posters on the wall, all edge networks highlight the presence of those objects, being EdgeNet more precise. This also happened on the fifth row, where EdgeNet has identified the window while other models have not.

The second row of Figure 5 depicts some problems re-

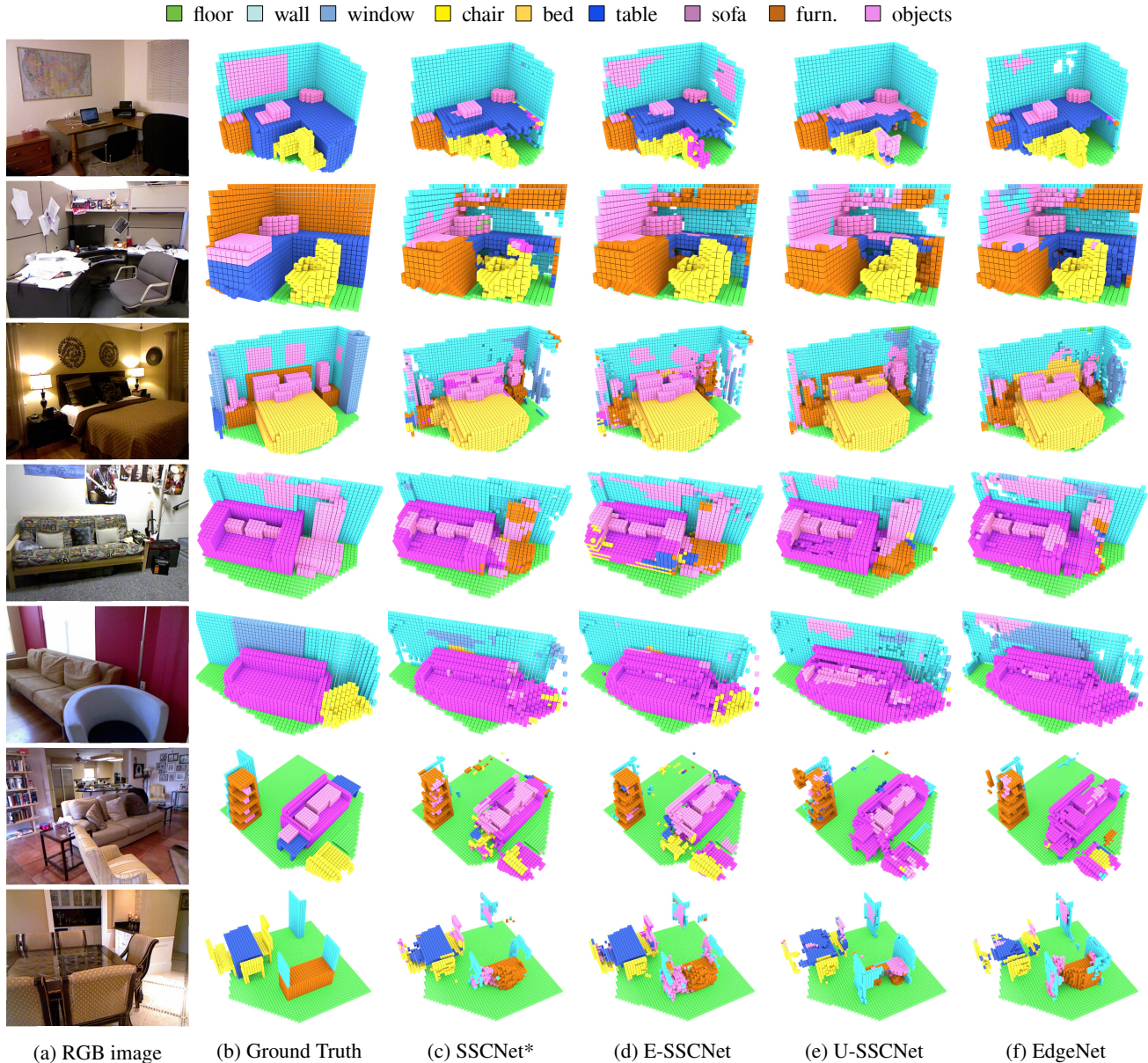


Figure 5: **Qualitative Results.** We compare our results (EdgeNet) with scene completion results from Song *et al.* [25] on SUNCG and NYU. Overall, EdgeNet gives more accurate voxel predictions (best viewed in colour).

model	Scene Completion			avg. SSC IoU
	prec.	rec.	IoU	
SSCNet*	79.4	64.6	55.3	30.8
U-SSCNet	76.3	69.1	56.8	31.0
E-SSCNet	77.8	66.4	55.8	31.0
EdgeNet	76.3	71.1	58.3	32.6

Table 3: **Overall results of our models on NYU.** All models were trained on SUNCG and fine tuned on NYU.

lated to Ground Truth annotations on NYU dataset. Note that neither the papers fixed on the wall nor the shelf appear in the Ground Truth. Most of the models captured the shelf, but only EdgetNet inferred the presence of objects fixed on the wall. When quantitative results are computed, ground truth annotation flaws like these unfairly benefit the less precise models and harm more precise models like EdgeNet.

7. Discussion

In this section we discuss key aspects of our proposed approach.

7.1. Is aggregating edges helpful?

We compared the original SSCNet architecture with our modified version of it that aggregates edges encoded with F-TSDF (E-SSCNet). E-SSCNet presented better results on both SUNCG and NYU datasets. One could argue that this improvement is due to the new training pipeline, rather than the edge encoding. To verify this, we compared our EdgeNet with a version of it without edges (U-SSCNet), both trained using the same pipeline. The result confirms that EdgeNet is better.

7.2. Is a deeper U-shaped CNN helpful?

We compared the original SSCNet to U-SSCNet, which is a deeper, U-shaped network that uses only depth as input, and U-SSCNet achieved better results. Once again, to check if the improvement was due to the new training pipeline, we compared our EdgeNet with E-SSCNet, which is a shallower CNN, but which also uses edges. EdgeNet gave better results, confirming that a deeper U-shaped CNN is helpful.

7.3. Has the new training pipeline any influence over results?

We compared the results originally achieved by SSCNet to results of the version of it trained with our pipeline. On SUNCG we observed an improvement of more than 20% on semantic scene completion and more than 8% on scene completion. On NYU, we observed a slight improvement on semantic scene completion scores. Besides the improvements on model performance, the pipeline also contributed to reduce training time from 7 days to 4 days when training on SUNCG and from 30 ours to 6 hours when training on NYU. Another important advantage of our pipeline, compared to the original one used by SSCNet is that, as it is less memory intensive, it allowed us to use a larger batch size. E-SSCNet could be trained on a simple GTX 1080Ti (which has 11GB of memory), with a batch of size 4, whereas the original framework only allowed a batch size of 1 sample on the same hardware. Besides reducing training time, larger batch sizes enhance training stability, acting as a regularizer [23].

7.4. How does EdgeNet compare to other colour-based approaches

We have compared EdgeNet with the colour-based approach of [7] and EdgeNet presented better results. Other recent models that use colour information [6, 14] are not end-to-end. They have the drawback of using a two step training approach: first they require that a 2D segmentation

sub-network be trained and then the 3D CNN can be trained. SSCNet and our EdgeNet are end-to-end networks.

7.5. An issue with the training set

The edges used to train EdgeNet were extracted from a slightly different version of the SUNCG dataset than one used by [25] to generate depth maps and ground truth. We noticed that there are small differences in some scenes between the version of SUNCG used in [25] and the version v1 available for download, which causes some scenes to have a small misalignment in some objects when comparing generated RGB with original depth and Ground Truth. In some instances, movable objects lead to greater differences. For instance, there are scenes where the depth map was generated with a door closed and that door appears opened in the RGB image. We believe that using the same version to extract GT, depth and edges will lead to some improvement, but unfortunately this version was not available for download by the time of our experiments. This issue has not affected the competing works that combined depth and RGB for Semantic Scene Completion because they have not used the same training set from SUNCG as the original SSCNet paper [25].

8. Conclusion

This paper presented a new approach to fuse depth and colour into a CNN for semantic scene completion. We introduced the use of F-TSDF encoded 3D projected edges extracted from RGB images. We also presented a new end-to-end network architecture capable of properly aggregating edges and depth and extracting useful information from both sources, with no requirement for previous 2D semantic segmentation training as previous depth plus colour approaches. Experiments with alternate models, showed that both aggregating edges and the new proposed architecture have positive impact on semantic scene completion, especially in hard to detect objects. Qualitative results show visually perceptible improvements in 3D label inferences and we have achieved improvement over the state-of-the-art result on the NYU depth v2 dataset, for end-to-end approaches.

We developed a lightweight training pipeline for the task, which reduced the memory footprint in comparison to the original implementation of SSCNet and reduced the training time on SUNCG from 7 to 4 days and on NYU from 30 to 6 hours.

For future work, we propose the use of domain adaptation techniques to transform the synthetic training images so that their appearance becomes more similar to that of the real indoor scenes observed in the target domain.

References

- [1] E. Aarts and J. Korst. *Simulated Annealing and Boltzmann Machines: A Stochastic Approach to Combinatorial Optimization and Neural Computing*. John Wiley & Sons, Inc., New York, NY, USA, 1989. 4
- [2] Y. Bengio, J. Louradour, R. Collobert, and J. Weston. Curriculum learning. In *Proceedings of the 26th Annual International Conference on Machine Learning, ICML '09*, pages 41–48, New York, NY, USA, 2009. ACM. 4
- [3] J. Canny. A computational approach to edge detection. *IEEE Transactions on Pattern Analysis and Machine Intelligence*, PAMI-8(6):679–698, Nov 1986. 3
- [4] L. Chen, G. Papandreou, I. Kokkinos, K. Murphy, and A. L. Yuille. Deeplab: Semantic image segmentation with deep convolutional nets, atrous convolution, and fully connected crfs. *IEEE Transactions on Pattern Analysis and Machine Intelligence*, 40(4):834–848, April 2018. 2
- [5] M. Firman, O. M. Aodha, S. Julier, and G. J. Brostow. Structured prediction of unobserved voxels from a single depth image. In *2016 IEEE Conference on Computer Vision and Pattern Recognition (CVPR)*, pages 5431–5440, June 2016. 1
- [6] M. Garbade, J. Sawatzky, A. Richard, and J. Gall. Two stream 3D semantic scene completion. *CoRR*, abs/1804.03550, 2018. 1, 2, 5, 8
- [7] A. B. S. Guedes, T. E. de Campos, and A. Hilton. Semantic scene completion combining colour and depth: preliminary experiments. *CoRR*, abs/1802.04735, 2018. 1, 2, 3, 5, 6, 8
- [8] R. Guo, C. Zou, and D. Hoiem. Predicting complete 3D models of indoor scenes. *CoRR*, abs/1504.02437, 2015. 5
- [9] Y. Guo and X. Tong. View-Volume Network for Semantic Scene Completion from a Single Depth Image. In *Proceedings of the Twenty-Seventh International Joint Conference on Artificial Intelligence*, pages 726–732, Stockholm, Sweden, July 2018. International Joint Conferences on Artificial Intelligence Organization. 2, 5
- [10] S. Gupta, P. Arbellez, and J. Malik. Perceptual organization and recognition of indoor scenes from rgb-d images. In *2013 IEEE Conference on Computer Vision and Pattern Recognition*, pages 564–571, June 2013. 1
- [11] A. Handa, V. Patraucean, V. Badrinarayanan, S. Stent, and R. Cipolla. Scenenet: Understanding real world indoor scenes with synthetic data. *CoRR*, abs/1511.07041, 2015. 5
- [12] K. He, X. Zhang, S. Ren, and J. Sun. Deep residual learning for image recognition. In *2016 IEEE Conference on Computer Vision and Pattern Recognition (CVPR)*, pages 770–778, June 2016. 3, 4
- [13] A. Janoch, S. Karayev, J. T. Barron, M. Fritz, K. Saenko, and T. Darrell. A category-level 3-d object dataset: Putting the kinect to work. In *2011 IEEE International Conference on Computer Vision Workshops (ICCV Workshops)*, pages 1168–1174, Nov 2011. 3
- [14] S. Liu, Y. HU, Y. Zeng, Q. Tang, B. Jin, Y. Han, and X. Li. See and think: Disentangling semantic scene completion. In S. Bengio, H. Wallach, H. Larochelle, K. Grauman, N. Cesa-Bianchi, and R. Garnett, editors, *Conference on Neural Information Processing Systems (NeurIPS)*, pages 263–274. Curran Associates, Inc., 2018. 3, 5, 8
- [15] J. Long, E. Shelhamer, and T. Darrell. Fully convolutional networks for semantic segmentation. In *2015 IEEE Conference on Computer Vision and Pattern Recognition (CVPR)*, pages 3431–3440, June 2015. 2
- [16] D. Marr. *Vision: A Computational Investigation into the Human Representation and Processing of Visual Information*. MIT Press, 1982. 1
- [17] D. T. Nguyen, B. Hua, M. Tran, Q. Pham, and S. Yeung. A field model for repairing 3D shapes. In *2016 IEEE Conference on Computer Vision and Pattern Recognition (CVPR)*, pages 5676–5684, June 2016. 1
- [18] X. Qi, R. Liao, J. Jia, S. Fidler, and R. Urtasun. 3D graph neural networks for RGBD semantic segmentation. In *IEEE International Conference on Computer Vision (ICCV)*, pages 5209–5218, 10 2017. 1
- [19] X. Ren, L. Bo, and D. Fox. Rgb-(d) scene labeling: Features and algorithms. In *2012 IEEE Conference on Computer Vision and Pattern Recognition*, pages 2759–2766, June 2012. 1
- [20] O. Ronneberger, P. Fischer, and T. Brox. U-net: Convolutional networks for biomedical image segmentation. In N. Navab, J. Hornegger, W. M. Wells, and A. F. Frangi, editors, *Medical Image Computing and Computer-Assisted Intervention – MICCAI 2015*, pages 234–241, Cham, 2015. Springer International Publishing. 2, 4
- [21] N. Silberman, D. Hoiem, P. Kohli, and R. Fergus. Indoor segmentation and support inference from rgb-d images. In A. Fitzgibbon, S. Lazebnik, P. Perona, Y. Sato, and C. Schmid, editors, *Computer Vision – ECCV 2012*, pages 746–760, Berlin, Heidelberg, 2012. Springer Berlin Heidelberg. 5
- [22] L. N. Smith. A disciplined approach to neural network hyper-parameters: Part 1 - learning rate,

- batch size, momentum, and weight decay. *CoRR*, abs/1803.09820, 2018. 4, 5
- [23] S. Smith, P. Jan Kindermans, C. Ying, and Q. V. Le. Don't decay the learning rate, increase the batch size. In *Sixth International Conference on Learning Representations (ICLR 2018)*, 2018. 8
- [24] S. Song, S. P. Lichtenberg, and J. Xiao. Sun rgb-d: A rgb-d scene understanding benchmark suite. In *2015 IEEE Conference on Computer Vision and Pattern Recognition (CVPR)*, pages 567–576, June 2015. 3
- [25] S. Song, F. Yu, A. Zeng, A. X. Chang, M. Savva, and T. Funkhouser. Semantic Scene Completion from a Single Depth Image. In *Conference on Computer Vision and Pattern Recognition (CVPR)*, 2017. 1, 2, 3, 4, 5, 6, 7, 8
- [26] J. Xiao, A. Owens, and A. Torralba. SUN3D: A database of big spaces reconstructed using SfM and object labels. In *2013 IEEE International Conference on Computer Vision*, pages 1625–1632, Dec 2013. 3
- [27] J. Zhang, H. Zhao, A. Yao, Y. Chen, L. Zhang, and H. Liao. Efficient semantic scene completion network with spatial group convolution. In *The European Conference on Computer Vision (ECCV)*, September 2018. 2, 6